ELSEVIER

Response of piles due to lateral slope movement

G.R. Martin [a], C.-Y. Chen [b],*

[a] *University of Southern California, CA, USA*
[b] *National Science and Technology Center for Disaster Reduction, Taipei, Taiwan*

Abstract

A displacement method using the FLAC^{3D} program is used to evaluate the response of piles caused by an embankment slope in a translational failure mode, induced by a weak soil layer or a liquefied layer beneath the embankment. The analyses include the kinematic loading acting on the bridge piles caused by lateral soil movements, and the effects of spatial variation of soil displacement on the response of piles and pile groups (2×2). The analysis demonstrates that the proposed displacement method can be applied to design of pile foundations undergoing lateral soil movement or for use in pile–slope stability analysis. Sensitivity studies varying soil and pile parameters are also presented. The results bring out the important effects of relative stiffness between pile and soil on the pile's failure modes. Published case histories are examined and used as a basis for verifying the proposed methodology.
© 2004 Elsevier Ltd. All rights reserved.

Keywords: Three-dimensional analysis; Passive pile; Finite difference; Lateral soil movement; Pile groups; Soil–pile interaction

1. Introduction

In the 1989 Loma Prieta Earthquake, one span of the San Francisco–Oakland Bay Bridge collapsed, induced by the translational movement of pile foundations associated with an embankment on soft soil [24]. During the 1995 Hyogoken-Nanbu Earthquake, a group of piles were damaged during the earthquake (before the superstructure was imposed) by a liquefaction induced lateral spread [6]. The piles were severely damaged at the interfaces between liquefied and non-liquefied layers. A pseudo-static analysis of the piles conducted by Tokimatsu and Asaka [21], without any vertical loading and inertial forces,

demonstrated the significant effects of lateral ground displacement on pile damage. Numerical analyses using the finite element program, DGPILE-3D, have shown that bending moments in the pile caused by lateral soil movement could be more significant than those caused superstructure loading [8]. The mechanics of representative displacement loading on piles from translational embankment failure on a weak or liquefied layer, is illustrated in Fig. 1.

2. Pile response analysis

Methods to analyze the pile response undergoing liquefaction induced lateral spread include full dynamic analysis, displacement response method and an uncoupled method. In the uncoupled method, pile–soil interaction is represented by equivalent Winkler or p–y springs.

* Corresponding author. Address: 3F, No. 106, Section 2, HoPing E. Road, Taipei 106, Taiwan.
E-mail address: chienyuc@ncdr.nat.gov.tw (C.-Y. Chen).

Nomenclature

c'	effective stress cohesion of soil	K_0	coefficient of earth pressure at rest
c_u	undrained shear strength	k_n, k_s	normal and shear stiffness of interface
$E_p I_p$	pile rigidity	N_{avg}	averaged standard penetration test
E_s	Young's modulus of soil	ρ	density of soil
G	shear modulus of soil	ϕ'	effective stress friction angle of soil
K	bulk modulus of soil	ψ	soil dilation angle

Forces acting on the spring are determined by free field displacements and imposed on the pile statically as external loading to evaluate the response of piles. That is, an uncoupled approach is used. The displacement method has demonstrated that we can get the same order of maximum moment on piles compared to a full system of dynamic analysis using finite element analysis [8], despite neglecting the inertial forces from the superstructure. A comparison between results of static analysis using GROUP [15] and full dynamic analysis using ADINA [1] and PAR [10] was conducted by Zechlin and Chai [24].

In this study, vertical loading and inertial forces from superstructure are not considered and only pile response caused by lateral soil movement is evaluated, as the effects of seismic inertial forces from a structure are less important for this case [18]. Kinematic forces induced by dynamic ground displacement are also not considered and only permanent ground displacement is considered as this is the dominant loading mechanism for large lateral spreads (e.g. [21, 23]). The numerical finite difference program FLAC[3D] (Fast Lagrangian Analysis of Continua in 3-Dimensions [7]) is used for the analysis. Utilizing the intrinsic FISH language allows the developed shear forces and reaction forces acting on the piles to be determined directly. Piles are formatted by a number of zones, but maintain elastic behavior during the lateral loading. Potential gapping between the pile/soil interface is incorporated using interface elements.

The concept used herein is similar to the method used by Poulos [11, 12, 13], Chen and Poulos [4] to evaluate the behavior of piles in an unstable slope. Reese et al. [16] also analyzed the loading induced by unstable slope movement as driving forces acting on stabilizing piles. The concept has also been used to design piled bridge foundations subjected to lateral spreads by CAL-TRANS (California Department of Transportation, http://www.dot.ca.gov/) in recent years. Published cases include the retrofitting of San Francisco–Oakland Bay Bridge [24] and the design of Charles River Bridge in Boston [19]. In the design of Charles River Bridge [19], the program LPILE 4.0 [17] was used to compute pile loads from lateral spreading. The force induced by a liquefied layer acting on piles was distributed as an external drag force. However, a case history analysis has shown that the drag forces acting on piles within a liquefied layer are often small relative to passive loading from the un-liquefied crust above the liquefied layer [2].

2.1. Pile grid spacing: Benchmark test

An elastic cantilever beam was initially analyzed to decide the vertical grids needed to attain reasonable numerical accuracy. The analysis applied a displacement on the top of the pile element shown in Fig. 2(a) to simulate a 12 m length of pile that is subjected to lateral loading on a pile cap. Shear forces developed during lateral loading are calculated directly by summation the total forces along the specified pile section. The shear force for each pile section is calculated from the product of the horizontal shear stresses and the area of each small zone. The area of each small zone is obtained from the volume of each zone divided by the length of each element segment. Results of numerical analysis are compared with the elastic solution by back-calculating the displacement at the top of the pile.

Higher vertical zone numbers in pile elements, provide for more flexibility to catch the characteristics of bending behavior. Pile sections for conducted analyses were fixed with 80 zones and vertical grid numbers are added up to 60 with a constant shear forces distribution along the pile shaft and with a maximum error of approximately 6% (Fig. 2(b)). While the pile tip was not fixed in the following analyses, minimum vertical grids are decided once shear forces tended to be constant in the analyses.
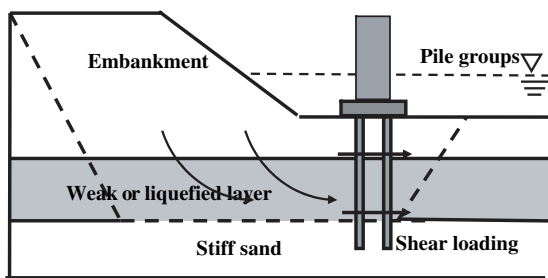

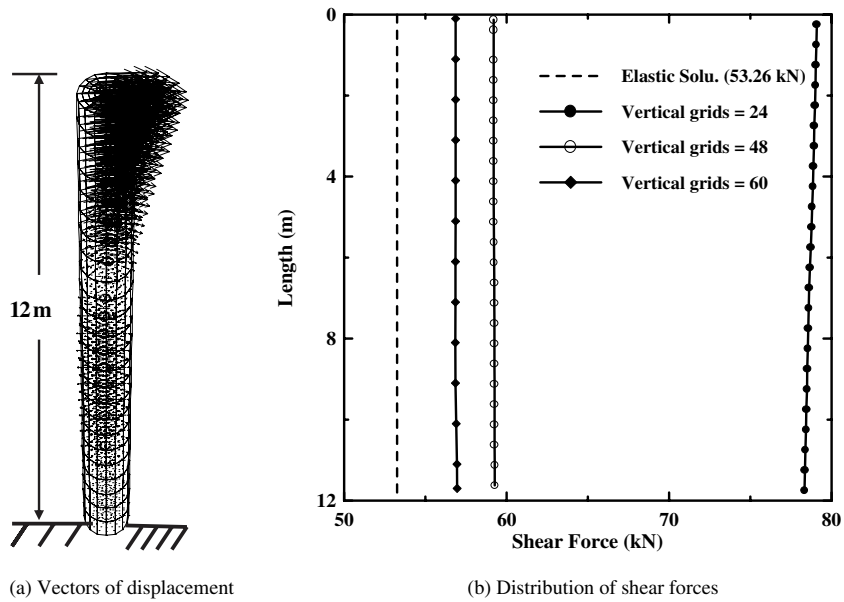Fig. 1. Shear loading acting on bridge piles caused by lateral soil spreading.

(a) Vectors of displacement

(b) Distribution of shear forces

Fig. 2. Elastic cantilever beam test.

2.2. Single pile behavior under lateral spread displacements: test case

For simplification, a uniform distribution of soil movement is assumed and applied on both sides of boundaries along the direction of soil movement as shown in Fig. 3, although the maximum displacement often occurs at an intermediate elevation in a liquefied or weak layer which is the seat of lateral spread movement.

The properties of the single pile and soil parameters used are indicated in Table 1. Both stable and weak soil masses are modelled as an elasto-plastic Mohr–Coulomb material with a tension cut-off. The middle 4 m weak layer has a lower residual strength assigned. Pile length is 12 and 1 m in diameter. A rough pile/soil interface is used, with normal (k_n) and shear (k_s) stiffness equal to 10^5 kN/m. Water table is kept constant at the ground surface. The free field displacement was applied 6 m from the outer boundary to the center of pile.
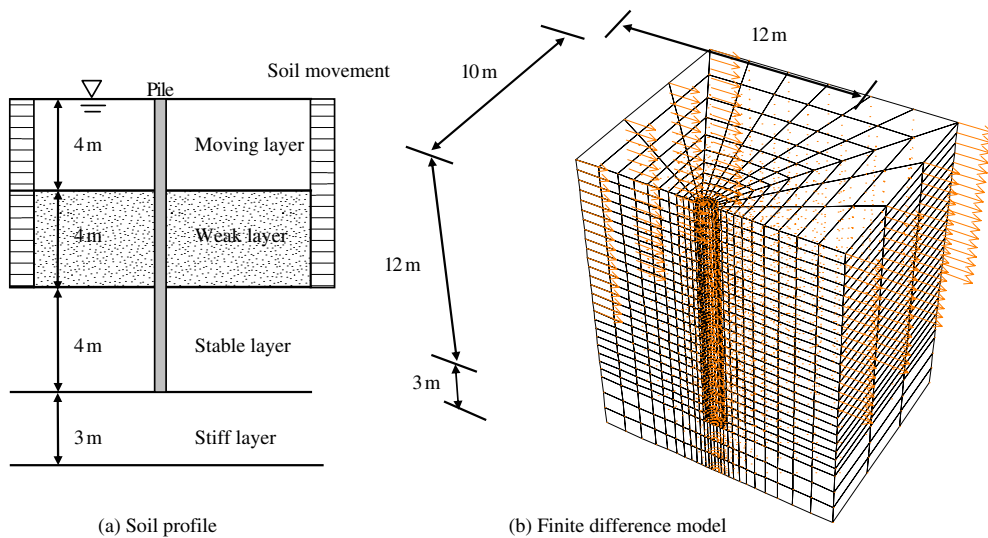

(a) Soil profile

(b) Finite difference model

Fig. 3. Single pile undergoing lateral soil movements.

Table 1
Material parameters used in the piles undergoing lateral soil movements

| Material	K (GPa)	G (GPa)	c (kPa)	ϕ (deg)	ψ (deg)	ρ (kg/m³)	K_0
Pile	13.9	10.4	–	–	–	2500	–
Moving layer	0.2	0.1	0	30	0	2000	1.0
Weak layer	0.2	0.1	0	20	0	2000	1.0
Stable layer	0.2	0.1	0	30	0	2000	1.0

Uniform soil movement from the ground surface down to the bottom of the weak layer is assumed (type A movement). The 1 m diameter of pile has $E_pI_p = 1230$ MN m² (equivalent to a Poisson ratio 0.2, a shear modulus 10.4 GPa and a bulk modulus 13.9 GPa), which represents a reinforced concrete pile.

Fig. 4(a)–(c) shows the distribution of pile deflections, shear forces and bending moments along the pile length, respectively. Lateral soil movements up to 60 mm at two sides of the boundaries were applied. An additional trapezoidal displacement profile (type B movement) was also applied. The maximum shear force
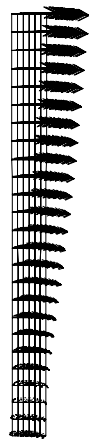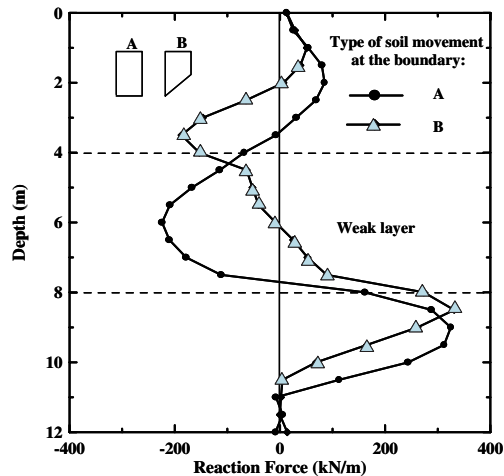

(a) Magnified pile displacement vectors under type A of soil movement
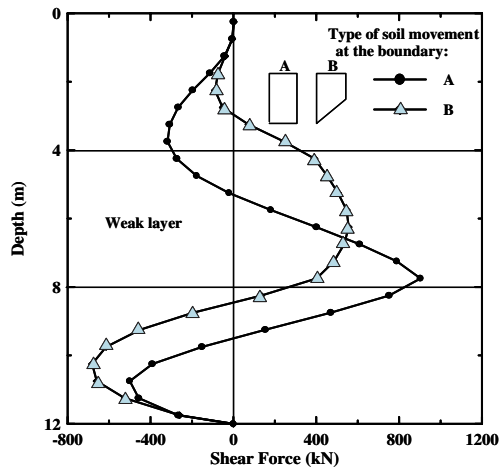
(b) Shear force developed on single pile
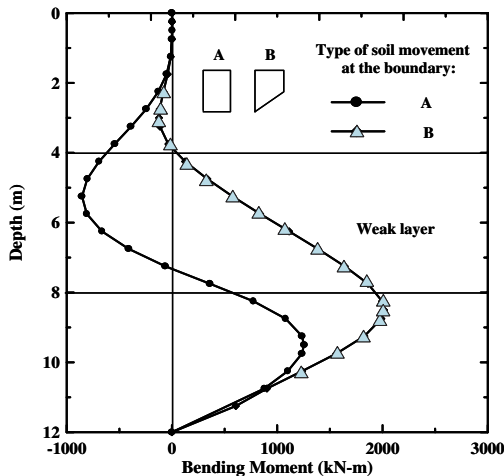
(c) Bending moment developed on single pile

(d) Forces on Single Pile Undergoing Lateral Soil Movement

Fig. 4. Response of single pile undergoing lateral soil movements.

developed within the pile shaft is close to the position of interface between stable and sliding masses. The distribution of bending moment along the pile shaft is obtained indirectly by integration the area of the shear force diagram. Bending moments are taken as zero at the top and bottom of the pile. The maximum bending moment in the pile was located within the stable soil.

2.3. Lateral load on pile

Fig. 4(d) depicts the reaction forces along on the pile shaft at the end of soil movement. The lateral load on a specified pile node is summed from the forces along the direction of soil movements acting on the interface nodes at the same level and the shear drag loading on both sides of the pile shaft. It should be noted that the lateral loads on the piles varied during the process of soil movement. Reaction force or driving force on the pile depends on the relative displacement between pile and soil. Once the soil movements exceed the pile deflection, then they will cause driving forces on the pile shaft.

3. Parametric studies

To clarify soil and pile parameters effecting pile–soil interaction during lateral spreads, a sensitivity study was conducted. The parameters considered include the pile bending stiffness, the effects of a soil strength reduction, and pile group effects. Details of parametric studies are present by Chen [5].

3.1. Effect of pile bending stiffness

The effects of pile bending stiffness are evaluated by a change in pile bending stiffness from $E_pI_p = 1230\,\mathrm{MN\,m^2}$ to $10E_pI_p$ and $0.1E_pI_p$. These changes could reflect different types or diameters of piles, and the possibility of cracks in reinforced concrete piles. Fig. 5 shows the change in pile deflections (under the same lateral soil movements as the uniform case in former section) with the varying pile bending stiffness. When the pile bending stiffness was higher than E_pI_p, the pile deflection was higher than soil movement and the failure mode was defined as the "intermediate mode" as defined by Poulos [14]. A softer pile bending stiffness ($0.1E_pI_p$) gave pile deflections close to the soil movement. This is referred to as "short pile mode". Development of pile bending moment within the pile shaft with varying of pile bending stiffness is depicted in Fig. 6. Higher pile bending stiffness leads to undergo higher shear force and bending moment in the stable soil mass.

Soil pressures acting on the pile are shown in Fig. 7. The softer pile bending stiffness caused a lowering of lateral load acting on the pile shaft, but when pile bending stiffness was higher than E_pI_p, forces acting on the pile
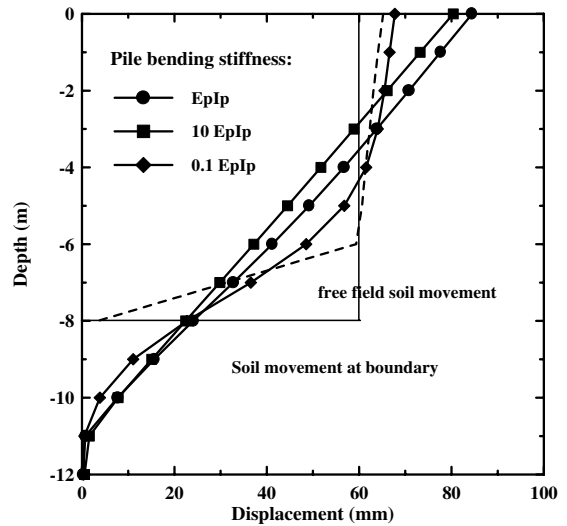
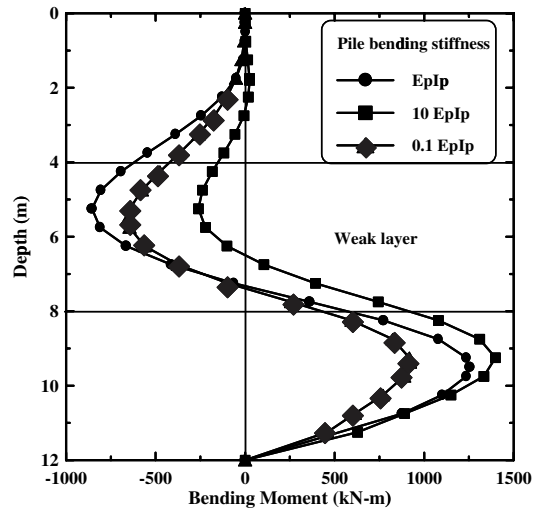Fig. 5. Effect of pile bending stiffness on pile deflection.

Fig. 6. Effect of pile bending stiffness on development of pile bending moment.

did not increase. This trend implies that soil plastic flow occurred around the pile shaft.

3.2. Effect of soil strength reduction on response of piles

The former analysis was based on a nominal residual strength of the weak layers simulating for example, a silt layer using the Mohr–Coulomb model. In theory, soil strength could reduce with the development of plastic strain during soil movement for sensitive clays or silts. To better simulate the process of strain softening, the intrinsic strain-softening model in FLAC[3D] was adopted for the weak layer for a comparison. The
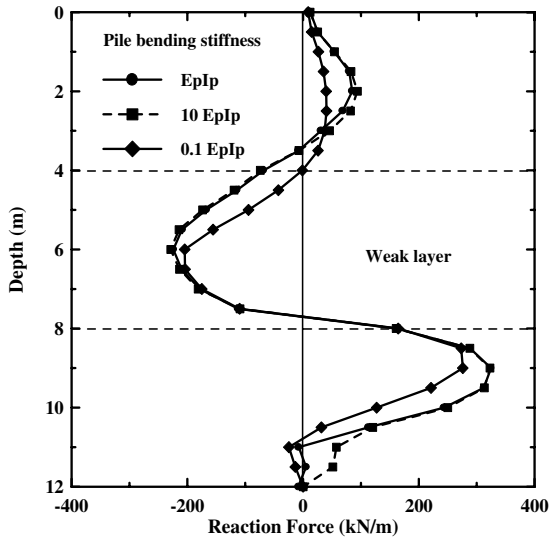
Fig. 7. Effect of pile bending stiffness on development of soil reaction on pile.
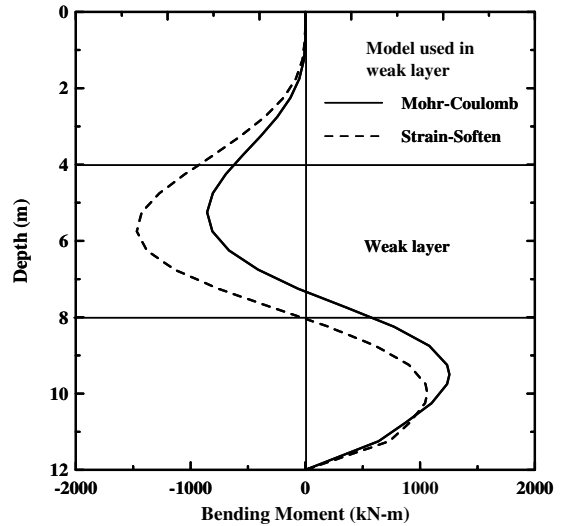

Fig. 9. Effect of soil constitutive model on development of pile bending moment.

strain-softening model is based on the principles of the Mohr–Coulomb model while allowing the change of soil strength parameters to vary with the increment of plastic strain. The variation of the friction angle in the weak layer with an increment of plastic strain used is shown in Fig. 8. The weak layer has a friction angle of 26° before strain softening but has a residual strength of 20° after strain softening, which is same as used for the original example. Results of the bending moment on the pile are shown in Fig. 9, respectively. Surprisingly, the strain-softening model results in higher pile response within the unstable soil mass but a smaller response in
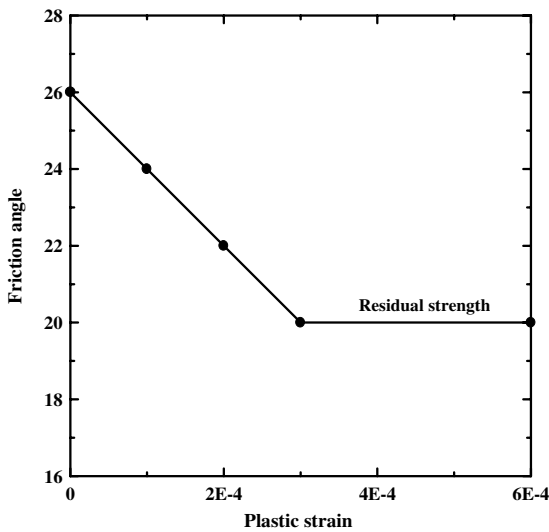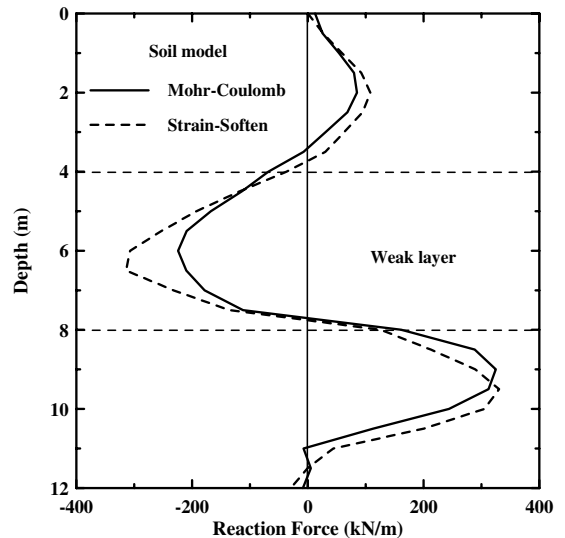

Fig. 10. Effect of soil constitutive model on development of reaction force on pile.

the stable soil. However, the soil reaction forces on the pile within the stable soil have similar values (Fig. 10).

4. Pile groups (2 × 2)

The response of a pile group (2 × 2) with a pile cap to lateral soil movement without any superstructure inertial forces are shown in Fig. 11. Two cases are analyzed: One is pile cap resting on the ground surface and the
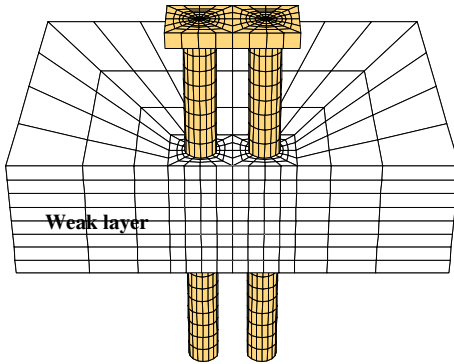

Fig. 8. Variation of friction angle with plastic strain.

Fig. 11. Pile groups (2 × 2) undergoing lateral soil movement.

Fig. 13. Distribution of shear force on pile groups.

other is a pile cap embedded in the ground surface. All material parameters and soil lateral movement conditions are same as the former single pile analysis test case. Fig. 12 shows the magnified pile deflection pattern for 60 mm of uniform lateral soil movement at both sides of the boundary. Uplift forces on the bottom of the pile cap caused higher vertical displacements on the leading piles than the trailing piles.

4.1. Effect of pile head constraint

Field observations show that piles may crack at the pile head and cap connection due to inertial forces from superstructures [21]. To illustrate the contribution of shear loading on the pile cap caused by weak layer deformation, the pile group was free of superstructure (e.g., without inertial forces) external forces.

The constraint of the embedded pile cap caused the piles to develop smaller shear forces and bending moments than the single isolated pile. The contribution of shear loading induced by lateral soil movements on interaction at the pile head and cap are one-tenth of
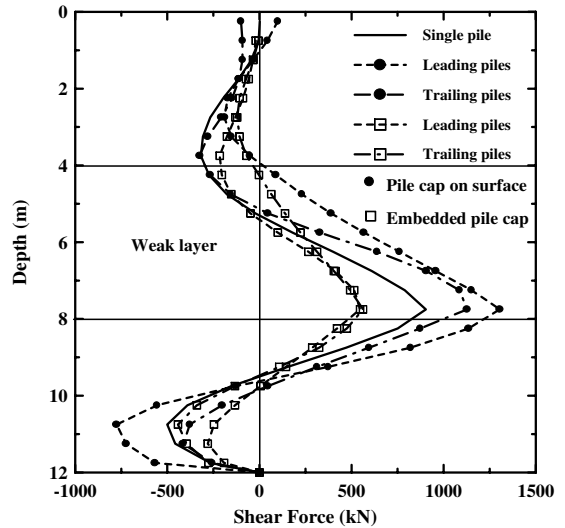
the maximum shear loading within the weak layer as shown in Fig. 13 in the case of pile cap on the ground surface. Distribution of bending moment is plotted in Fig. 14. Group piles for both the leading and trailing piles revealed higher bending moments than the single pile within the stable soil in the case of pile cap on the ground surface. For the case of embedded pile cap, significant of passive loading at the pile cap induced by soil movement causes a smaller of pile response than the single pile behavior.

5. Validation of the numerical scheme

One case history analyzed by Meyersohn et al. [9] and the other case history calibrated by Chen and Poulos [4]

(a) Pile capon the ground surface   (b) Pile cap embedded in the ground
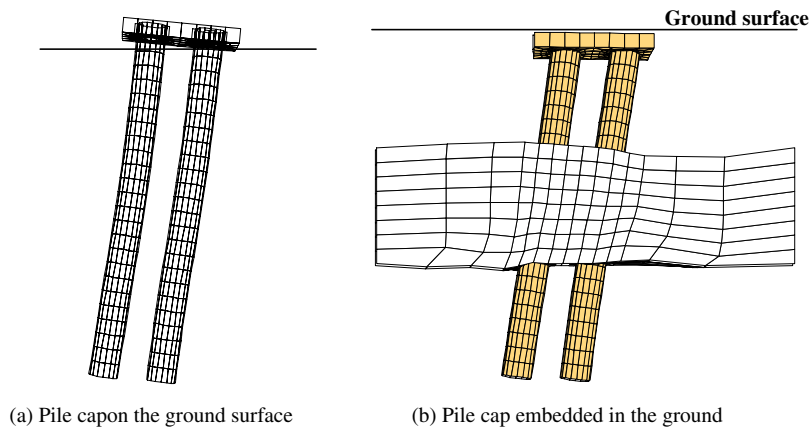
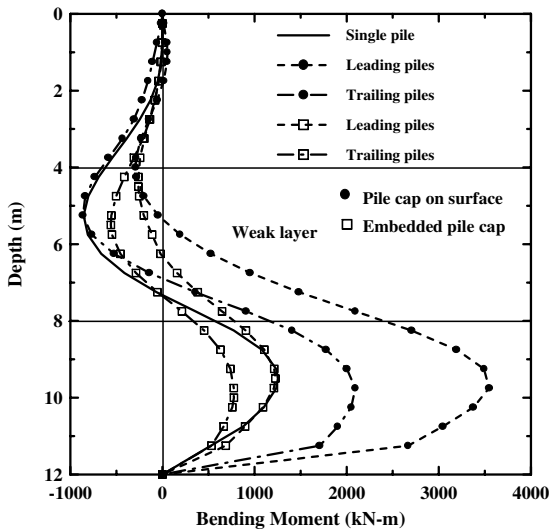Fig. 12. Magnified displacement of pile groups (20 times).

Fig. 14. Distribution of bending moment on pile groups.

were used to verify the accuracy of numerical tools used for simulating pile response under lateral soil movement.

5.1. Case 1 NHK building

Meyersohn et al. [9] analyzed a pile supported building subjected to earthquake lateral spread using the computer program B-STRUCT. The B-STRUCT program uses a Winkler spring assumption for soil–pile interaction, similar to LPILE. The reinforced concrete piles had a diameter of 35 cm, and were 11 m in length. Pile damage was revealed after field excavation as shown in Fig. 15(a). Serious cracks were observed at 2.5–3.5 m from the ground surface and 2–3 m from the pile tip. Since soil liquefied at a depth 3–8.5 m from ground surface, the postulated soil movement was taken as uniform
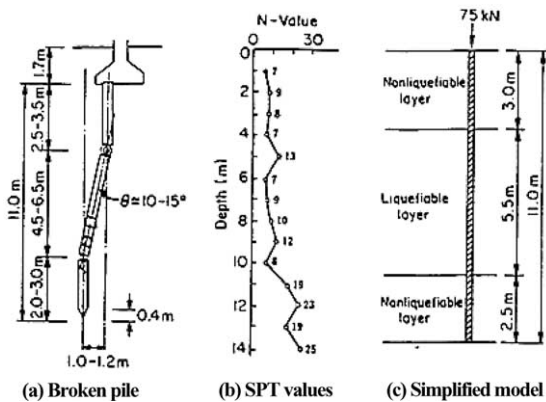
from surface to the top of liquefied layer with a linear increase from the bottom of the liquefied layer to the top. Moving soils had a friction angle of 32° and a unit weight of 16.7 kN/m^3. Liquefied soil had a residual friction angle of 1°, based on the estimation of 1/50 reduction ratio of the Meyersohn et al. [9] analysis. Dense sand in the stable base had a friction angle 40° and a unit weight of 17.6 kN/m^3. Soil SPT-N values are depicted in Fig. 15(b).

To compare the analyzed results from FLAC^{3D} and B-STRUCT, the soil Young's modulus was assumed as uniform with a value estimated from the average SPT-N value of $E_s = 1.0N_{avg}$ which is equivalent to 10^3 kPa ($N_{avg} = 9$). Pile stiffness E_pI_p was estimated as 18.4 MN m^2. A rough interface with normal and shear stiffness equal to 10^5 kN/m was used. The simplified model used followed the analysis model of Meyersohn et al. [9] as shown in Fig. 15(c). The vertical force (75 kN) from the superstructure was converted into stresses acting on the pile top.

The finite difference grid used as well as the vectors of applied lateral soil movements in the finite difference analysis is shown in Fig. 16. The calculated distributed shear forces along the pile shaft are shown in Fig. 17 for intact soil strength and reduced liquefied residual strength. Potential positions of plastic hinges are around 8.5 and 3.5 m below the ground surface, which coincide with the failure mode of the pile. Pile deflections and soil movements are shown in Fig. 18. The distribution of bending moment as depicted in Fig. 19 shows that the pile yielded first at the lower interface between the liquefied and un-liquefied layer. The lower liquefied layer

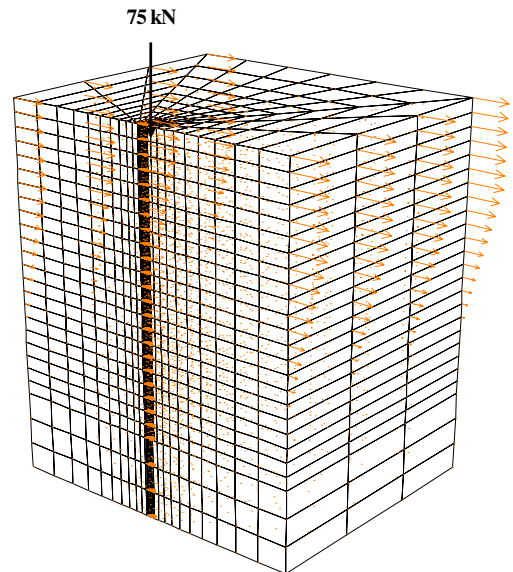Fig. 15. Schematic of typical damaged pile at NHK building (after 9).

Fig. 16. Finite difference zones and vectors of lateral soil movements at the NHK building site.
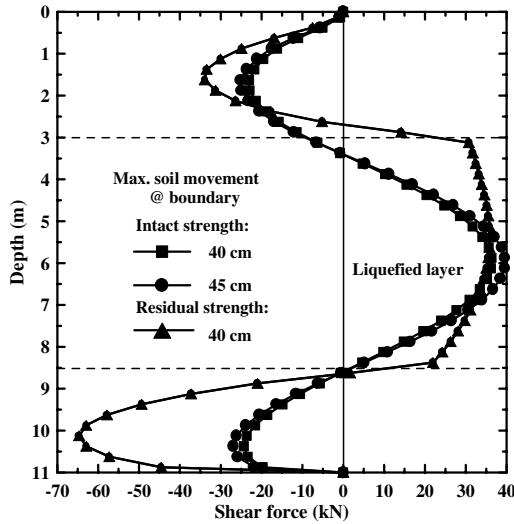
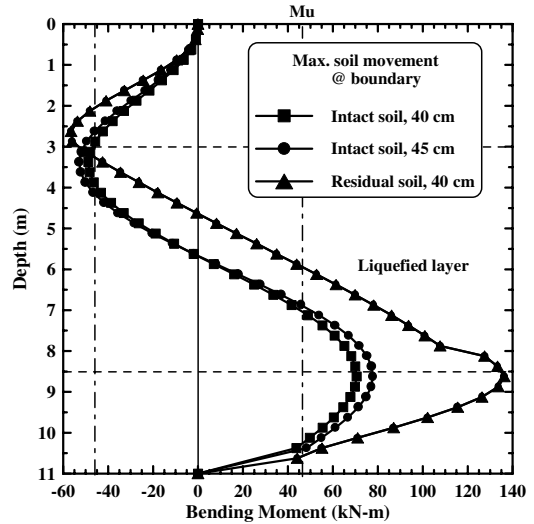Fig. 17. Analytical result of pile shear force at the NHK building site.

Fig. 18. Pile deflection and soil movements from the modelling of the NHK building foundation.

Fig. 19. Analytical result of pile bending moment at the NHK building site.

strength caused higher pile bending moments at the lower interface. This is inconsistent with the analyses result of Stewart et al. [20], which showed that the values of liquefied residual strength had minor effect under this type of soil movement. The effect of inertial force from superstructure was not considered. Whereas field observations from the 1995 Hyogoken-Nambu earthquake revealed that inertial force could cause the damage near the pile heads, damage adjacent to liquefied layers was due to the kinematic force from the liquefied layer [22].

The results of analysis suggested that the second plastic hinge developed as lateral soil movement approached 40 cm, which is lower than the result of B-STRUCT analysis. Estimation of distributed Young's modulus, and the number of vertical pile grids could be a factor causing the difference.

5.2. Case 2 full scale test

In this case history [3], a slope stabilizing reinforced concrete pile was 22 m long and 1.2 m in diameter. A plastic hinge at 12.5 m below the surface developed when the pile was subjected to a 9.5 m thickness of upper layer slope movement. The undrained shear strength of both the moving and stable soil layers was 30 kPa, as estimated by unconsolidated undrained triaxial tests. Chen and Poulos [4] estimated values of $E_s = 15$ MPa (e.g., $500c_u$) and $E_pI_p = 2035.8$ MN m^2 to match the measured bending moment. Nevertheless, in the case, the estimated soil Young's modulus was beyond the suggested value of $150c_u$ to $400c_u$ [4]. It was assumed that soil movement was uniform from the surface down to 9.5 m, with a value of 95 mm.

In the FLAC^{3D} analysis, the distance of applied displacements for the analysis was 10 m from boundary to the center of pile. Soil Young's modulus was estimated as $E_s = 200c_u = 6$ MPa, since $E_s = 500c_u$ was found to overestimate the piles response. A rough interface with normal and shear stiffness equal to 10^5 kN/m was used in the modelling. Results of the analysis are under the condition of a lateral soil displacement of 95 mm at the boundary. Fig. 20 plots the results for developed bending moment. Soil pressure on the pile is shown in Fig. 21 and the pile deflection is shown in Fig. 22. Soil
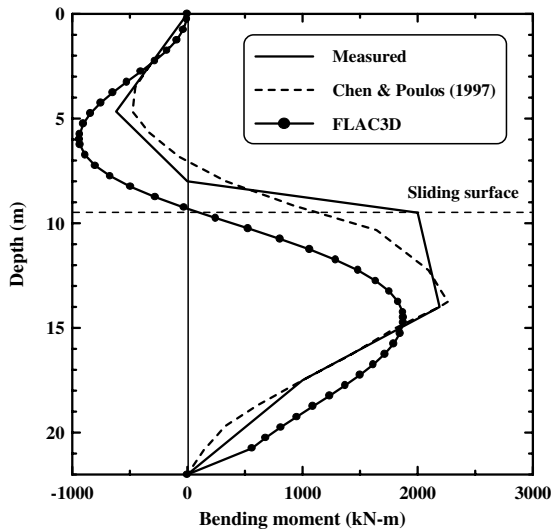
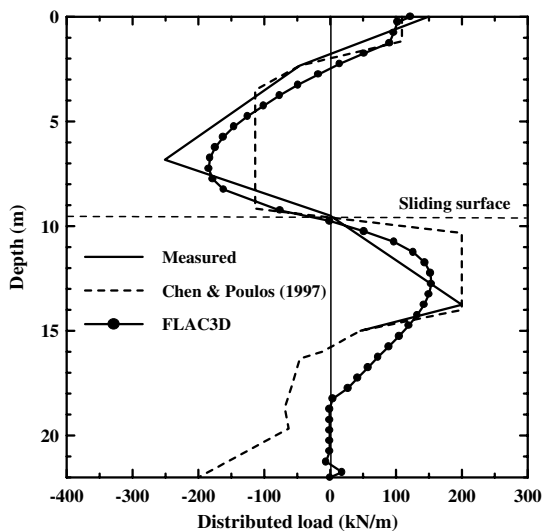Fig. 20. Distribution of bending moment from the full scale test.

Fig. 21. Distributed load on pile from the full scale test.

response over the stable soil was underestimated. Soil pressures on the pile shaft were also lower than the measured values, which implied the possibility of underestimating the Young's modulus. However the trend of the pile response is similar to observed values.

The type of displacement control could cause lower plastic hinge positions. Since uniform soil strength was used, the sliding surface at the interface between sliding and stable soil masses cannot be well defined. Other factors, in addition to the differences in modelling field conditions, such as the number of vertical grids in the pile and the soil Young's modulus used also have considerable effect on the pressures on the pile.
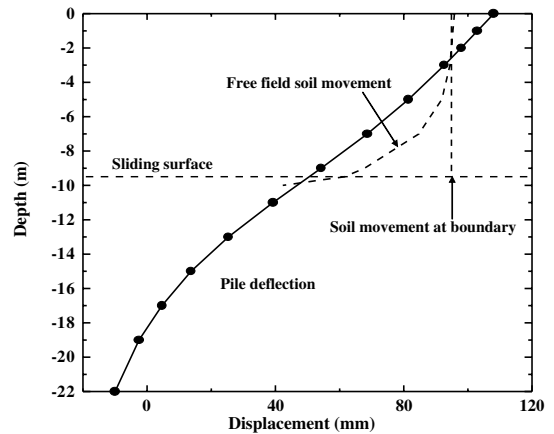

Fig. 22. Pile deflection and soil movements from the modelling of full scale test.

6. Conclusion

The results of the FLAC^{3D} finite difference analyses demonstrate its possibility to analyze the response of piles undergoing lateral soil spreading. In addition to effects of Young's modulus on response, sensitivity studies on soil and pile parameters showed that the relative stiffness between the pile and soil are important factors in determining the failure modes of the pile and the pressure (reaction force or driving loading) on the pile. The relative depth of displacing soil and stable soil is not the only factor deciding the failure mode of the passive piles. The methodology can be extended to design of piles in bridge embankments for example, subjected to lateral spreads and pile–slope stability analysis in which piles are used and need to be designed for slope stabilization.

References

[1] Bathe KJ. ADINA, automatic dynamic incremental nonlinear analysis. Users Manual, ADINA R&D; 1996.

[2] Berrill JB, Christensen SA, Keenan RJ, Okada W, Pettinga JR. Lateral-spreading loads on a piled bridge foundation. In: Seismic behaviour of ground and geotechnical structures. Rotterdam: Balkema; 1997. p. 173–83.

[3] Carrubba P, Maugeri M, Motta E. Esperienze in vera grandezza sul comportamento di pali per la stabilizzaaione di un pendio. In: Proceedings of the XVII Convegno Nazionale di Geotechica, vol. 1. Italiana: Assn. Geotec.; 1989. p. 81–90.

[4] Chen LT, Poulos HG. Piles subjected to lateral soil movements. J Geotech Geoenviron Eng, ASCE 1997; 123(9):802–11.

[5] Chen CY. Numerical analysis of slope stabilization concepts using piles. PhD thesis, University of Southern California; 2001.

[6] Horikoshi K, Ohtsu H. Investigation of PC piles damaged by the Hyogoken-Nanbu earthquake. In: Proceedings of the 31st Japan National Conference on Geotechnical Engineering, vol. 1. 1996. p. 1227–8.

[7] Itasca, FLAC³ᴰ. Fast Lagrangian analysis of continua in 3-dimensions. Version 2.0, Manual, Minneapolis, MN: Itasca; 1997.

[8] Kimura M, Zhang F. Seismic evaluations of pile foundations with three different methods based on three-dimensional elasto-plastic finite element. Soils Found 2000;40(5):113–32.

[9] Meyersohn WD, O'Rourke TD, Miura F. Lateral spread effects on reinforced concrete pile foundations. In: Fifth US–Japan workshop on earthquake disaster prevention for lifeline system, Tsukuba, Japan, October 26–30, 1992.

[10] PAR, pile analysis routines. Users Manual, San Francisco, CA: PMB Engineering, Inc.; 1995.

[11] Poulos HG. Behavior of laterally loaded piles: I—single piles. J Soil Mech Found Div, ASCE 1971;97(SM5):711–31.

[12] Poulos HG. Behavior of laterally loaded piles: II—pile groups. J Soil Mech Found Div, ASCE 1971;97(SM5):733–51.

[13] Poulos HG. Analysis of piles in soil undergoing lateral movement. J Soil Mech Found Div, ASCE 1973;99(SM5):391–405.

[14] Poulos HG. Design of reinforcing piles to increase slope stability. Can Geotech J 1995;32:808–18.

[15] Reese LC, Wang ST, Awoshika K, Lam PHF. Documentation of Computer Program GROUP. Version 2.0; 1990.

[16] Reese LC, Wang ST, Fouse JL. Use of drilled shafts in stabilizing a slope. In: Stability and performance of slopes and embankments—II. Geotechnical special publication no. 31, vol. 2. ASCE; 1992. p. 1318–32.

[17] Reese LC, Wang TS. Documentation of Computer Program LPILE. Version 4.0, Austin, TX: Ensoft, Inc.; 1993.

[18] Sasaki Y, Towhata I, Tokida KI, Yamada K, Matsumoto H, Tamari Y et al. Mechanism of permanent displacement of ground caused by seismic liquefaction. Soils Found 1992;32(3):79–96.

[19] Soydemir C, Kraemer SR, Davidson WA, LaPlante KE. Geotechnical-earthquake engineering design of Charles River Bridges in Boston. In: Geotechnical earthquake engineering and soil dynamics III. Geotechnical special publication no. 75, vol. 2. ASCE; 1998. p. 1235–46.

[20] Stewart HE, Miura F, O'Rourke TD. Pile damage due to large ground displacement. In: Proceedings, 1st Japan–US workshop on liquefaction, large ground deformations, and their effect on lifeline facilities, Tokyo, Japan, November 1988. p. 173–82.

[21] Tokimatsu K, Asaka Y. Effects of liquefaction-induced ground displacements on pile performance in the 1995 Hyogoken-Nambu earthquake. Soils Found 1998;2:163–77. [special issue].

[22] Tokimatsu K, Oh-oka H, Satake K, Shamoto Y, Asaka Y. Effects of lateral ground movements on failure patterns of piles in the 1995 Hyogoken-Nambu earthquake. In: Geotechnical earthquake engineering and soil dynamics III. Geotechnical special publication no. 75, vol. 2. ASCE; 1998. p. 1175–86.

[23] Towhata I, Orense RP, Toyota H. Mathematical principles in prediction of lateral ground displacement induced by seismic liquefaction. Soils Found 1999;39(2):1–19.

[24] Zechlin ET, Chai J. Nonlinear dynamic analysis of large diameter pile foundations for the Bay Bridge. In: Geotechnical earthquake engineering and soil dynamics III. Geotechnical special publication no. 75, vol. 2. ASCE; 1998. p. 1223–34.